

## Production of ozone and nitrogen oxides by laser filamentation

PETIT, Yannick, *et al.*

### Abstract

We have experimentally measured that laser filaments in air generate up to  $10^{14}$ ,  $3 \times 10^{12}$ , and  $3 \times 10^{13}$  molecules of  $O_3$ ,  $NO$ , and  $NO_2$ , respectively. The corresponding local concentrations in the filament active volume are  $10^{16}$ ,  $3 \times 10^{14}$ , and  $3 \times 10^{15} \text{ cm}^{-3}$ , and allows efficient oxidative chemistry of nitrogen, resulting in concentrations of  $HNO_3$  in the parts per million range. The latter forming binary clusters with water, our results provide a plausible pathway for the efficient nucleation recently observed in laser filaments.

PETIT, Yannick, *et al.* Production of ozone and nitrogen oxides by laser filamentation. *Applied physics letters*, 2010, vol. 97, no. 2, p. 021108

DOI : 10.1063/1.3462937

Available at:

<http://archive-ouverte.unige.ch/unige:37113>

Disclaimer: layout of this document may differ from the published version.





## Production of ozone and nitrogen oxides by laser filamentation

Yannick Petit, Stefano Henin, Jérôme Kasparian, and Jean-Pierre Wolf

Citation: [Applied Physics Letters](#) **97**, 021108 (2010); doi: 10.1063/1.3462937

View online: <http://dx.doi.org/10.1063/1.3462937>

View Table of Contents: <http://scitation.aip.org/content/aip/journal/apl/97/2?ver=pdfcov>

Published by the [AIP Publishing](#)

---



## Re-register for Table of Content Alerts

Create a profile.



Sign up today!



## Production of ozone and nitrogen oxides by laser filamentation

Yannick Petit, Stefano Henin, Jérôme Kasparian,<sup>a)</sup> and Jean-Pierre Wolf  
*GAP Biophotonics, Université de Genève, 20 rue de l'École de Médecine, CH1211 Genève 4, Switzerland*

(Received 4 June 2010; accepted 21 June 2010; published online 15 July 2010)

We have experimentally measured that laser filaments in air generate up to  $10^{14}$ ,  $3 \times 10^{12}$ , and  $3 \times 10^{13}$  molecules of  $O_3$ ,  $NO$ , and  $NO_2$ , respectively. The corresponding local concentrations in the filament active volume are  $10^{16}$ ,  $3 \times 10^{14}$ , and  $3 \times 10^{15}$   $cm^{-3}$ , and allows efficient oxidative chemistry of nitrogen, resulting in concentrations of  $HNO_3$  in the parts per million range. The latter forming binary clusters with water, our results provide a plausible pathway for the efficient nucleation recently observed in laser filaments. © 2010 American Institute of Physics.  
 [doi:10.1063/1.3462937]

In their propagation through transparent media, ultrashort laser pulses can generate self-guided filaments.<sup>1–4</sup> Filamentation stems from a dynamic balance between Kerr self-focusing on one side, and defocusing by both higher-order (negative) Kerr terms,<sup>5</sup> and the free electrons originating from the ionization of the propagation medium by the pulse itself. Filaments, which can be longer than 100 m,<sup>6</sup> be initiated remotely<sup>7</sup> and propagate through clouds<sup>8</sup> and turbulence,<sup>9</sup> are ideally suited for atmospheric applications<sup>4,10</sup> like lightning control,<sup>11</sup> or laser-assisted water nucleation.<sup>12</sup>

In subsaturated atmospheres, the latter effect cannot be explained by the Wilson mechanism<sup>13</sup> in which the charges stabilize charge-transfer complexes of  $H_2O^+O_2^-$ , on which droplets grow. Rather, the observed effect may imply binary nucleation of  $HNO_3$ ,<sup>14–16</sup> which according to the extended Köhler theory stabilizes the growing droplets of binary mixtures, similar to observations in cloud chambers for binary  $H_2SO_4-H_2O$ .<sup>17,18</sup> Assessing this pathway requires a precise knowledge of the physicochemistry of the filaments. In this paper, we measure the generation of three key gases, namely  $O_3$ ,  $NO$ , and  $NO_2$  by laser filaments. Filaments produce large amounts of these trace gases, allowing efficient oxidative chemistry of nitrogen and resulting in concentrations of  $HNO_3$  in the multiparts per million range, which may account for the efficient droplet nucleation induced by laser filaments in sub-saturated atmospheres.<sup>12</sup>

The experiments (Fig. 1) were conducted on the Helvetiera platform, which delivered laser pulses of up to 12 mJ energy and 80 fs Fourier-limited duration (150 GW peak power) at a wavelength of 800 nm and 100 Hz repetition rate. A chopper reduced this rate by a factor of 40 in most experiments (i.e., an average of 2.5 pulses/s) to limit the concentration in the cell and reduce the chemical reactions between the generated species as well as to avoid saturation of the measurement devices. The incident pulse duration was varied by detuning the laser compressor to induce a chirp. The beam ( $2 \times 2.4$  cm cross section) was focused by an  $f=2.8$  m lens to generate one to two filaments in a 2 m long Plexiglass cell of 2 cm diameter with 250  $\mu m$  thin fused silica windows. Fresh air from the room entered freely the cell at one of its ends. At its other end, the air was continuously pumped in parallel through polyethylene tubes by an

ozone analyzer (Horiba APOA-350E) at a flow of 2.2 l/min and a NOx analyzer (Monitor laboratories 8840) at a flow of 0.5 l/min. Although in the filaments, ozone and NOx are partly ionized, the transit time of  $\sim 10$  s through the sampling circuit ensures that they are neutralized before entering the analyzers, so that ionized species are measured together with neutral ones.

All measurements were performed once steady state was reached in the cell. We checked that all measurements were linear with the number of laser shots per unit time. If we neglect chemical reactions among the NOx and  $O_3$  during the transit to the analyzers, the variation in the measured concentration  $C_i$  of species  $i$  depends on the generation of this species by the laser beam (source term  $S_i$ ) and its dilution by the flow  $F$  through the cell.

$$V \times dC_i/dt = S_i - F \times C_i. \quad (1)$$

In a steady state, the source term reads the following:

$$S_i = C_i \times F. \quad (2)$$

Volumic generation rates and the resulting concentrations are then evaluated by dividing  $S_i$  by the total filament volume, corresponding to two filaments of 0.5 m length and of 100  $\mu m$  diameter, i.e., a total volume of 4  $mm^3$ . In Eqs. (1) and (2), we have neglected the losses and source terms due to chemical reactions, especially the oxidation of  $NO$  and  $NO_2$  by ozone<sup>17</sup>



as well as on the walls of the cell, mainly the degradation of ozone into  $O_2$  on the wall surface, as follows:

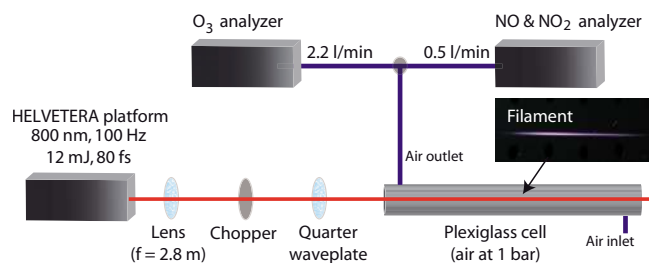


FIG. 1. (Color online) Experimental setup.

<sup>a)</sup>Electronic mail: jerome.kasparian@unige.ch.

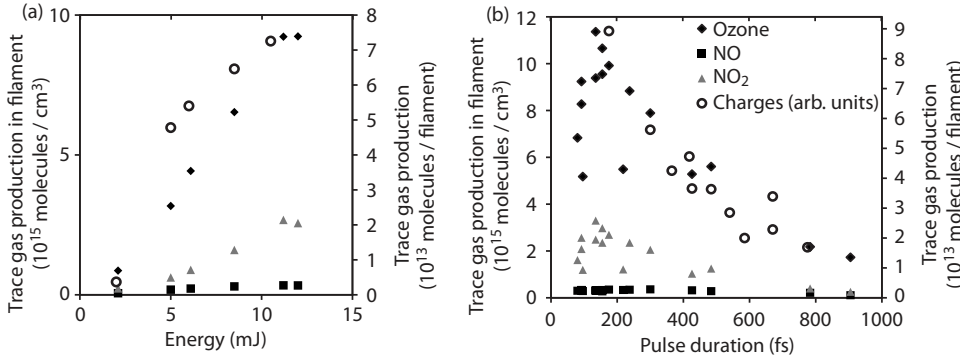


FIG. 2. Generation of O<sub>3</sub>, NO, and NO<sub>2</sub> in laser filaments as a function of (a) the incident energy for a pulse duration of 80 fs and (b) the pulse duration for a pulse of 11.2 mJ energy.



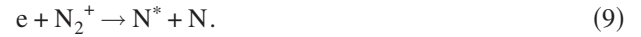
We, therefore, measure a lower limit for the production of O<sub>3</sub> and NO by the laser filaments. On the other hand, the effect on NO<sub>2</sub> is more complex, since Reactions (3) and (4) have opposite effects. These contributions are discussed at the end of the present manuscript. In parallel with the concentration of trace gases, we measured the relative efficiency of charge release by the filaments, as detailed in Ref. 19.

Figure 2 displays the generation rate per unit volume of O<sub>3</sub>, NO, and NO<sub>2</sub> in the filament as a function of the incoming pulse energy and duration. Obviously, the filaments produce considerable amounts of these trace gases. For 2.5 shots/s, the concentrations averaged over the cell volume reach 200 ppb of O<sub>3</sub> and 50 ppb of NO<sub>2</sub>, one order of magnitude above typical atmospheric values and even higher than the alert level in most countries. They correspond to the generation of extremely high concentrations within the filament volume: 400 ppm (10<sup>16</sup> cm<sup>-3</sup>) of ozone and 100 ppm of NO<sub>2</sub> (3 × 10<sup>14</sup> cm<sup>-3</sup>), respectively.

The production of O<sub>3</sub>, NO, and NO<sub>2</sub> increases quite linearly with pulse energy, with a threshold between 1 and 2 mJ, corresponding to the filamentation threshold in our experimental conditions. It is proportional to that of electrons for various pulse durations and energies (Fig. 2). Linearly polarized pulses yield 19% more ozone, 33% more NO, and 68% more NO<sub>2</sub>, consistent with the fact that a linear polarization is more favorable to filamentation than a circular one,<sup>20</sup> resulting, in our setup, in twice as much charge generation than circularly polarized pulses. These data show that NOx and ozone are mainly produced in the filaments, hence in plasma, rather than in the photon bath. The corresponding pathways may therefore be activated by photodissociation, ionization, or electron impact onto O<sub>2</sub> and N<sub>2</sub> molecules. The very complex chemistry occurring in air plasmas<sup>21,22</sup> prevents us to isolate one single scheme, although three of them are more likely to contribute significantly to the formation of NO. The first one relies on the N<sup>+</sup> ions, which are highly reactive with O<sub>2</sub>, with a rate constant as high as 5 × 10<sup>-10</sup> cm<sup>3</sup>/s at 300 K. Note that, throughout this work, we use of the rate constants at room temperature because the filaments are known to negligibly heat the heavy species of the plasma.<sup>2,3</sup> The branching ratios are 43%, 51%, and 6% between the reactions, as follows<sup>23</sup>:



Alternatively, the recombination of electrons with N<sub>2</sub><sup>+</sup>, can break the N–N bond and lead to the following<sup>24</sup>:



The excited nitrogen atom can also be generated by the following<sup>21</sup>:



The activated nitrogen atoms will then react with oxygen molecules, as follows:



Besides Reactions (6) and (11), O<sup>\*</sup> is also produced by the following<sup>25</sup>



The oxygen atoms immediately react with oxygen molecules, as follows:



Ozone will then oxidize NO into NO<sub>2</sub> through reaction (3). Although the main reaction paths are identified above, simulations of the measured concentrations using rate equations is currently impossible because of the very riche chemical dynamics at play<sup>21</sup> and of the lack of data on the initial N<sup>\*</sup>, N<sub>2</sub><sup>\*</sup>, N<sup>+</sup>, and N<sub>2</sub><sup>+</sup> concentrations in the filaments. However, since the concentration of O<sub>3</sub>, NO, and NO<sub>2</sub> are closely related to that of the electrons, a process initiation by Reactions (6)–(9) is more likely than (10). The very high concentrations O<sub>3</sub> and NO<sub>2</sub> in the filament volume allow an efficient chemistry. In particular, the equilibrium<sup>17</sup>



is governed by  $K_{14} = [\text{N}_2\text{O}_5] / ([\text{NO}_2][\text{NO}_3]) = 3 \times 10^{-11}$  cm<sup>3</sup> at 298 K. N<sub>2</sub>O<sub>5</sub> immediately reacts with water, as follows:



Given the rate constant  $k_4 = 3 \times 10^{-17}$  cm<sup>3</sup>/s of Reaction (4),<sup>17</sup> the extremely high NO<sub>2</sub> and ozone concentrations in the filaments could generate up to 6 × 10<sup>14</sup> molecules/cm<sup>3</sup>/s of NO<sub>3</sub>, a production rate comparable with that of NO<sub>2</sub> in our experiments. Considering the equilibrium constant K<sub>14</sub> and the reaction rate  $k_{15} = 3 \times 10^{-4}$  s<sup>-1</sup>, Reactions (4), (14), and (15) clearly result in the generation of N<sub>2</sub>O<sub>5</sub>, hence HNO<sub>3</sub>, in the parts per million range, or even higher. Binary HNO<sub>3</sub>–H<sub>2</sub>O clusters<sup>16</sup> then form, grow into condensation nuclei and allow macroscopic

droplet formation and net uptake of water from the atmosphere. Reactions (6)–(15) provide a large excess of condensation nuclei as compared with the droplet densities of at most some  $10^3 \text{ cm}^{-3}$  observed in our recent nucleation experiments.<sup>12</sup> Chemistry therefore appears as the dominant process in laser-induced condensation in subsaturated atmospheres. At least, that relevant species are available in amounts largely sufficient to explain the observed condensation.

Up to now, we have neglected the losses due to Reactions (3)–(5). Since all species are generated simultaneously, their concentrations can be considered as roughly proportional (as is also visible on Fig. 2) so that the reaction rates depend on the square of the considered concentration. Under this assumption, the rate Eq. (1) rewrites, for each species  $i$ , as follows:

$$V \times dC_i/dt = S_i - k_i C_i^2 - FC_i, \quad (16)$$

so that in the steady state,

$$C_i = (-F + \sqrt{F^2 + 4k_i S_i})/2k_i. \quad (17)$$

Comparing results in two conditions with identical source term and different pumping rates (hence, sampling flows) yields

$$k_i = (C_{i,1}F_1 - C_{i,2}F_2)/(C_{i,2}^2 - C_{i,1}^2). \quad (18)$$

In the case of ozone, we measured  $[O_3]_1=314$  ppb for  $F_1=2.2$  l/min and  $[O_3]_2=285$  ppb for  $F_2=2.7$  l/min, which yields  $k_{O_3}=4.5$  l/min/ppm. Implementing this correction increases the source term by at most 10%: the losses due to ozone depletion via chemical processes in the flow cell is not the main source of error. Furthermore,  $[NO_2]_1=124$  ppb for  $F_1=0.5$  l/min and  $[NO_2]_2=32$  ppb for  $F_2=2.7$  l/min, result in  $k_{NO_2}=1.7$  l/min/ppm, so that the correction is limited to 1.3%, showing that the main sources and sinks of  $NO_2$ , i.e., respectively Reactions (3) and (4), approximately balance each other. Losses due to chemistry therefore affect little our measurements of both  $NO_2$  and  $O_3$ . These effects are of the same order of magnitude or larger than the long-term drift of the gas analyzers over the time span of the measurements. The concentrations at the output of the cell, and hence the production rates of  $O_3$  and  $NO_2$  (right scales in Fig. 2) can therefore be trusted within typically 10%. On the other hand, the molecule concentrations in the filament volume (left scale in Fig. 2) rely on the estimation of typical filament diameters,<sup>1–4</sup> which may be trusted within a factor of 2. However, the excess of  $HNO_3$  by orders of magnitudes as compared to the amounts required to explain the observed laser-induced water condensation<sup>12</sup> ensures the validity of our qualitative conclusion in spite of this relatively large quantitative uncertainty.

The depletion of NO was estimated by considering the rate  $k_3=1.9 \times 10^{-14} \text{ cm}^3/\text{s}$  of Reaction (3) (Ref. 17) and the concentration retrieved in the filaments. We find a depletion rate  $d[NO]/[NO]dt=k_3 \times [O_3]=200 \text{ s}^{-1}$ . As a consequence, the NO produced is almost completely oxidized into  $NO_2$  within 50 ms due to the extremely high ozone concentration. This confirms that Reaction (3) is far from being the limiting factor in the generation of  $HNO_3$ .

As a conclusion, we have experimentally measured that laser filaments in air generate up to  $10^{14}$ ,  $3 \times 10^{12}$ , and  $3 \times 10^{13}$  molecules of  $O_3$ , NO, and  $NO_2$ , respectively. The

corresponding local concentrations in the filament active volume are  $10^{16}$ ,  $3 \times 10^{14}$ , and  $3 \times 10^{15} \text{ cm}^{-3}$  and allow efficient oxidative chemistry of nitrogen, resulting in concentrations of  $HNO_3$  in the parts per million range. The latter forming binary clusters with water, our results provide a plausible pathway for the efficient nucleation observed in laser filaments, especially in subsaturated atmospheres.

We gratefully acknowledge B. Lazarrotto (Service de la Protection de l'Air de Geneve) for supplying the trace gas analyzers. This work was supported by the Swiss NSF (Contract No. 200021-125315).

<sup>1</sup>S. L. Chin, S. A. Hosseini, W. Liu, Q. Luo, F. Theberge, N. Akozbek, A. Becker, V. P. Kandidov, O. G. Kosareva, and H. Schroeder, *Can. J. Phys.* **83**, 863 (2005).

<sup>2</sup>A. Couairon and A. Mysyrowicz, *Phys. Rep.* **441**, 47 (2007).

<sup>3</sup>L. Bergé, S. Skupin, R. Nuter, J. Kasparian, and J.-P. Wolf, *Rep. Prog. Phys.* **70**, 1633 (2007).

<sup>4</sup>J. Kasparian and J.-P. Wolf, *Opt. Express* **16**, 466 (2008).

<sup>5</sup>P. Béjot, J. Kasparian, S. Henin, V. Lorient, T. Vieillard, E. Hertz, O. Faucher, B. Lavorel, and J.-P. Wolf, *Phys. Rev. Lett.* **104**, 103903 (2010).

<sup>6</sup>B. La Fontaine, F. Vidal, Z. Jiang, C. Y. Chien, D. Comtois, A. Desparois, T. W. Johnson, J.-C. Kieffer, and H. Pépin, *Phys. Plasmas* **6**, 1615 (1999).

<sup>7</sup>M. Rodriguez, R. Bourayou, G. Méjean, J. Kasparian, J. Yu, E. Salmon, A. Scholz, B. Stecklum, J. Eislöffel, U. Laux, A. P. Hatzes, R. Sauerbrey, L. Wöste, and J.-P. Wolf, *Phys. Rev. E* **69**, 036607 (2004).

<sup>8</sup>G. Méjean, J. Kasparian, J. Yu, E. Salmon, S. Frey, J.-P. Wolf, S. Skupin, A. Vinçotte, R. Nuter, S. Champeaux, and L. Bergé, *Phys. Rev. E* **72**, 026611 (2005).

<sup>9</sup>R. Salamé, N. Lascoux, E. Salmon, J. Kasparian, and J. P. Wolf, *Appl. Phys. Lett.* **91**, 171106 (2007).

<sup>10</sup>J. Kasparian, M. Rodriguez, G. Méjean, J. Yu, E. Salmon, H. Wille, R. Bourayou, S. Frey, Y.-B. André, A. Mysyrowicz, R. Sauerbrey, J.-P. Wolf, and L. Wöste, *Science* **301**, 61 (2003).

<sup>11</sup>J. Kasparian, R. Ackermann, Y.-B. André, G. Méchain, G. Méjean, B. Prade, P. Rohwetter, E. Salmon, K. Stelmaszczyk, J. Yu, A. Mysyrowicz, R. Sauerbrey, L. Wöste, and J.-P. Wolf, *Opt. Express* **16**, 5757 (2008).

<sup>12</sup>P. Rohwetter, J. Kasparian, K. Stelmaszczyk, S. Henin, N. Lascoux, W. M. Nakaema, Y. Petit, M. Queißer, R. Salamé, E. Salmon, Z. Q. Hao, L. Wöste, and J.-P. Wolf, *Nat. Photonics* **4**, 451 (2010).

<sup>13</sup>W. Byers Brown, *Chem. Phys. Lett.* **235**, 94 (1995).

<sup>14</sup>V.-M. Kerminen, A. S. Wexler, and S. Potukuchi, *J. Geophys. Res.* **102**, 3715 (1997).

<sup>15</sup>T. Koop, B. Luo, U. M. Biermann, P. J. Crutzen, and T. Peter, *J. Phys. Chem. A* **101**, 1117 (1997).

<sup>16</sup>F. Yu, *Atmos. Chem. Phys.* **6**, 5193 (2006).

<sup>17</sup>J. H. Seinfeld and S. N. Pandis, *Atmospheric Chemistry and Physics—From Air Pollution to Climate Change*, 2nd ed. (Wiley, New York, 2006).

<sup>18</sup>J. Duplissy, M. B. Enghoff, K. L. Aplin, F. Arnold, H. Aufmhoff, M. Avngaard, U. Baltensperger, T. Bondo, R. Bingham, K. Carslaw, J. Curtis, A. David, B. Fastrup, S. Gagné, F. Hahn, R. G. Harrison, B. Kellert, J. Kirkby, M. Kulmala, L. Laakso, A. Laaksonen, E. Lillestol, M. Lockwood, J. Mäkelä, V. Makhmutov, N. D. Marsh, T. Nieminen, A. Onnela, E. Pedersen, J. O. P. Pedersen, J. Polny, U. Reichl, J. H. Seinfeld, M. Sipilä, Y. Stozhkov, F. Stratmann, H. Svensmark, J. Svensmark, R. Veenhof, B. Verheggen, Y. Viisanen, P. E. Wagner, G. Wehrle, E. Weingartner, H. Wex, M. Wilhelmsson, and P. M. Winkler, *Atmos. Chem. Phys.* **10**, 1635 (2010).

<sup>19</sup>S. Henin, Y. Petit, D. Kiselev, J. Kasparian, and J.-P. Wolf, *Appl. Phys. Lett.* **95**, 091107 (2009).

<sup>20</sup>G. Fibich and B. Ilan, *Phys. Rev. E* **67**, 036622 (2003).

<sup>21</sup>I. A. Kossyi, A. Yu. Kostinsky, A. A. Matveyev, and V. P. Silakov, *Plasma Sources Sci. Technol.* **1**, 207 (1992).

<sup>22</sup>H. L. Xu, A. Azarm, J. Bernhardt, Y. Kamali, and S. L. Chin, *Chem. Phys.* **360**, 171 (2009).

<sup>23</sup>I. Dotan, P. M. Hierl, R. A. Morris, and A. A. Viggiano, *Int. J. Mass Spectrom. Ion Process.* **167–168**, 223 (1997).

<sup>24</sup>J. N. Bardsley, *J. Phys. B* **1**, 365 (1968).

<sup>25</sup>O. V. Braginskij, A. N. Vasilieva, K. S. Klopovskiy, A. S. Kovalev, D. V. Lopaev, O. V. Proshina, T. V. Rakhimova, and A. T. Rakhimov, *J. Phys. D: Appl. Phys.* **38**, 3609 (2005).